Click Here for Full Article

Estimation of mixing in the troposphere from Lagrangian trace gas reconstructions during long-range pollution plume transport

I. Pisso,[1,2,3] E. Real,[2,4] K. S. Law,[2] B. Legras,[3] N. Bousserez,[5,6] J. L. Attié,[5,7] and H. Schlager[8]

[1]   The dispersion and mixing of pollutant plumes during long-range transport across the North Atlantic is studied using ensembles of diffusive backward trajectories in order to estimate turbulent diffusivity coefficients in the free troposphere under stratified flow conditions. Values of the order of $0.3-1$ m^2 s^{-1} and 1×10^4 m^2 s^{-1} for the vertical and horizontal diffusivity coefficients D_v and D_h, respectively, are derived. Uncertainties related to the method are discussed, and results are compared with previous estimates of atmospheric mixing rates. These diffusivity estimates also yield an estimate of the vertical/ horizontal aspect ratio of tracer structures in the troposphere. Results from this case study are used to estimate grid resolutions needed to accurately simulate the intercontinental transport of pollutants as being of the order of 500 m in the vertical and at least 40 km in the horizontal. This work forms the basis of high-resolution chemical simulations using ensembles of diffusive backward trajectories.

1.   Introduction

[2]   Simulations of global atmospheric composition designed to investigate climate change and regional air quality issues rely on numerical models of transport and chemistry. This requires accurate simulation of the long-range transport of pollutants from source to receptor regions. Observations have shown that, downwind from emission regions, where pollutants are uplifted into the free troposphere by convection or frontal systems, differential advection, due to stratification, reduces the scale of tracer structures leading to the formation of narrow sheet-like layers downwind from continents occupying a significant volume of the troposphere [*Newell et al.*, 1999]. The variability of tropospheric mixing on small scales plays an important role in the distribution of such layers [*Colette and*

Ancellet, 2006]. The ability of global Eulerian models to simulate the intercontinental transport of pollutant layers is governed largely by the spatial resolution of the simulations. Current computational constraints generally limit global chemical transport models (CTMs) to spatial scales of 1° or greater, with trace gas concentrations assumed constant in model grid boxes. Mixing tends to be overestimated in such coarse resolution models with effective horizontal diffusivities, related to spurious numerical diffusion, leading to the smearing out of small-scale features [*Tan et al.*, 1998]. In addition, chemical rates, calculated from mean grid values ignore any subgrid scale variability and correlations between species which can result in systematic errors in CTM trace gas budgets [*Pyle and Zavody*, 1990; *Wu et al.*, 2007] which will be aggravated in case of nonlinear chemical reactions. Such systematic errors have been reported for ozone (O_3) [*Wild and Prather*, 2006], NO_x [*Cook et al.*, 2007], OH [*Crowther et al.*, 2002] and ClO_x [*Edouard et al.*, 1996; *Tan et al.*, 1998]. Other critical issues include the representation of emissions [*Sillman et al.*, 1990; *Esler et al.*, 2004] and subgrid scale processes such as convection. Model estimations of O_3 are clearly sensitive to such processes and the resolution of the simulations [*Wild and Prather*, 2006] but global models have yet to be tested at resolutions where they reach the limits dictated by small-scale turbulence in the atmosphere.

[3]   Small-scale structures can be explicitly represented in a Lagrangian framework, which separates advection by the flow from the effects of chemistry and mixing [*Methven et al.*, 2003]. Trajectory calculations are able to simulate more accurately the fine-scale structure created as air masses from

---

[1]Now at Department of Applied Mathematics and Theoretical Physics, University of Cambridge, Cambridge, UK.

[2]Service d'Aéronomie (LATMOS, UMR 7620), CNRS/IPSL/Université Pierre et Marie Curie, Paris, France.

[3]Laboratoire de Météorologie Dynamique (UMR 8539), CNRS/IPSL/ Ecole Normale Supérieure, Paris, France.

[4]Now at CEREA, Ecole Nationale des Ponts et Chaussées, Paris, France.

[5]Laboratoire d'Aérologie (UMR 5560), Université de Toulouse/CNRS, Toulouse, France.

[6]Now at Department of Physics and Atmospheric Science, Dalhousie University, Halifax, Nova Scotia, Canada.

[7]CNRM-GAME (URA 1357), Météo-France/CNRS, Toulouse, France.

[8]Institut für Physik der Atmosphäre, Deutsches Zentrum für Luft und Raumfahrt, Operpfaffenhofen, Germany.

different origins are brought into close proximity although individual trajectories may be subject to positional errors of ±20% [*Stohl et al.*, 2004, 2005]. Pure Lagrangian techniques neglect mixing yielding too large gradients [*Legras et al.*, 2003; *Methven et al.*, 2003], and do not represent chemical reactions leading to changes in concentrations within air parcels. In real atmospheric flows, the reduction in scale of filamentary structures combined with irreversible small-scale turbulence are efficient mixing processes, which are represented in models by a turbulent diffusivity tensor. In general, the horizontal component of the diffusivity, D_h, is several orders of magnitude larger than the vertical diffusivity, D_v due to quasi isentropic advection associated with strong stratification. This problem has been studied extensively in the stratosphere [*Hall and Waugh*, 1997; *Pisso and Legras*, 2008]. Different approaches have been developed to include mixing in Lagrangian models, i.e., based on local shear and strain in CLaMS [*McKenna et al.*, 2002] or ensemble random walks in TRACZILLA [*Legras et al.*, 2005]. In the troposphere, previous studies focused on estimating horizontal diffusivities of power plant or aircraft plumes [*Sillman et al.*, 1990; *Schumann et al.*, 1995].

[4] This paper forms the first part of a study designed to investigate the dynamical and chemical processes acting during long-range transport of a pollutant plume in the free troposphere. Here we focus on the quantification of plume dispersion during long-range transport and its relation to other mixing estimates including the "mixing" inherent in global models. We focus on the long-range transport of a forest fire plume during summer 2004 when fires were very active over Alaska and large amounts of trace gases such as carbon monoxide (CO) were emitted [e.g., *Pfister et al.*, 2005] providing an ideal tracer for investigating plume transport and dilution in the troposphere. Multiple aircraft samplings of the forest fire plume during transport from Alaska to western Europe are used to constrain estimations of vertical and horizontal diffusivities calculated using a stochastic Lagrangian reconstruction method previously applied in the stratosphere [*Pisso and Legras*, 2008]. These results, which allow quantification of dispersion rates of pollutant plumes in the troposphere, are compared to diffusion rates in three-dimensional CTMs, which are, as noted above, related to numerical diffusion at current resolutions. Results are also compared to other parameters used to describe plume dilution such as mixing rates estimated assuming an exponential decay to background concentrations [e.g., *Arnold et al.*, 2007; *Real et al.*, 2007].

[5] In a companion paper (E. Real et al., Novel high resolution modeling approach for the study of chemical evolution of pollutant plumes during long-range transport, submitted to *Journal of Geophysical Research*, 2009, hereinafter referred to as Real et al., submitted manuscript, 2009), the results presented here are used to perform high resolution photochemical calculations along multiple ensembles of trajectories originating every $15-30$ s along the flight tracks. This study examines the impact of multiple air mass origins on different parts of the plume samplings as well as the impact of transport versus photochemistry on trace gas distributions and correlations across the plume. Real et al. (submitted manuscript, 2009) also use the high resolution results to estimate local errors in net O_3 production

in global models related to chemical nonlinearities and spatial resolution.

[6] The data and methods used in this work are described in section 2. Estimates of vertical diffusivity from stochastic reconstructions in the troposphere and possible sources of error are presented in section 3. The accuracy of Lagrangian techniques representing large-scale advective processes affecting the quality of such reconstructions, in particular tracer gradient formation are discussed in section 4. The results are discussed and compared to previous mixing estimates in section 5. Estimates of the grid resolutions required for simulation of long-range transport in global CTMs are presented in section 6 and conclusions in section 7.

2. Data and Methods

2.1. The Lagrangian 2K4 Campaign

[7] During ICARTT (International Consortium for Atmospheric Research on Transport and Transformation), in summer 2004, a series of field experiments were conducted to study the processes influencing long-range transport of trace gases and aerosols across the North Atlantic from North America to Europe (see *Fehsenfeld et al.* [2006] for further details about flights and aircraft instrumentation). A Lagrangian pollutant experiment (International Global Atmospheric Chemistry (IGAC) Lagrangian 2K4) was performed with as many as six successful multiple samplings of the same air masses during transport across the North Atlantic [*Methven et al.*, 2006].

[8] One of these cases involved multiple samplings of a forest fire plume transported from Alaska to the west coast of Europe. This plume, clearly visible in MOPITT and AIRS CO data stretching over the North Atlantic [*Bousserez et al.*, 2007; *McMillan et al.*, 2008] may have been lofted into the free troposphere by convection triggered by the passage of a low pressure system following a dry and unusually warm period [*Damoah et al.*, 2006]. Subsequent transport in the free troposphere was largely advective and not influenced by convection making it a good case for study using the techniques employed in this study. The Lagrangian samplings by several aircraft have been analyzed in detail by *Methven et al.* [2006] (case 2) and *Real et al.* [2007]. Using backward and forward trajectory analysis and hydrocarbon fingerprint matching, *Methven et al.* [2006] identified Lagrangian matches between flight segments on the 18 July during a NASA DC8 flight over Newfoundland and a DLR (German Aerospace Center) Falcon flight on 23 July over the English Channel, five days later. Further trajectory analysis by *Real et al.* [2007] also showed a match between the DC8 plume on the 18 July and a DLR Falcon sampling on 22 July off the coast of Spain and southwest France. *Real et al.* [2007] also examined the processes responsible for the evolution of O_3 in the plume using a photochemical box model initialized with upwind observations. While photochemical production of O_3 due to PAN decomposition was important when the plume descended toward Europe, mixing with other air masses, based on the decrease of CO in the plume, was also shown to be an important factor governing trace gas evolution. These results are compared with this study in section 5.

2.2. Lagrangian Trajectory Calculations

[9] Atmospheric flows exhibit strongly stratified dynamics outside convective regions, as it is assumed to be the case in the long-range event studied here. Hence the main contribution to mixing comes from small-scale turbulent motion. This motivates the representation of small-scale turbulence in Lagrangian calculations as stochastic perturbations on the velocity field as a way of taking into account perturbations occurring at subgrid scales. It is assumed that the overall effect of turbulence in a spatial scale smaller than the grid of the advecting fields has timescales much smaller than the time step of advection, and hence can be approximated as a diffusive process. Due to the typical aspect ratio of atmospheric structures, this stochastic perturbation can be added either to the vertical or horizontal advecting winds.

[10] Reverse integrations of ensembles of trajectories initialized along the Lagrangian match segments of the flight tracks were performed with TRACZILLA [*Legras et al.*, 2003, 2005; *Pisso and Legras*, 2008]. This is a modified version of the trajectory model FLEXPART [*Stohl et al.*, 2005] which includes vertical or horizontal independent stochastic perturbations in the velocity field. The model was run using winds from the European Center for Medium Range Weather Forecasts (ECMWF) operational analysis at 1° horizontal resolution, and on 60 hybrid levels with 3-hour resolution obtained by combining analysis available every 6 hours with short time forecasts at intermediate times (3 hour resolution). One thousand parcels were initialized every second along the flight segments. CO concentrations from the CTM MOCAGE (MOdèle de Chimie Atmosphérique à Grande Echelle) (see next subsection) were mapped onto the backward endpoints of the trajectories, 4 to 9 days prior to the plume samplings. The stochastic perturbations associated with the turbulent diffusion in the vertical, D_v, or horizontal, D_h, applied to parcel positions, were varied in order to obtain the best agreement between stochastic reconstructions and the measured CO data along the flight tracks.

[11] These diffusive reconstructions, based on stochastic ensembles of backward trajectories, use dynamical information contained in the time series of advecting winds. This "zooming" translates this temporal information into increased spatial resolution of tracer fields from three-dimensional CTMs leading to improved agreement with fine scale features observed in the in situ measurements. Moreover, the resulting averaged vertical velocity helps to reduce uncertainties associated with the vertical velocity (ω) field.

2.3. MOCAGE

[12] Global CO fields from the MOCAGE three-dimensional CTM were used to initialize the multiple trajectory calculations. MOCAGE uses a semi-Lagrangian advection scheme [*Josse et al.*, 2004] to transport chemical constituents or tracers. The time step resolution is 15 min for chemical and physical processes and 60 min for dynamical processes. The horizontal grid resolution used in this simulation is 2×2 degrees. The model includes 47 hybrid ($\sigma - p$) levels from the surface to 5 hPa, corresponding to a vertical resolution of $40 - 400$ m in the boundary layer (7 levels) and about 800m around the tropopause. Turbulent diffusion follows the *Louis* [1979] scheme, while the

convection scheme (mass-flux type) is from *Bechtold et al.* [2001]. MOCAGE uses the chemical scheme RACMOBUS, which combines the REPROBUS scheme [*Lefèvre et al.*, 1994] for the stratosphere and the RACM scheme [*Stockwell et al.*, 1997] for the troposphere. RACMOBUS includes 119 individual species, among which 89 are prognostic variables, and 372 chemical reactions. The model also parameterizes dry deposition [*Nho-Kim et al.*, 2004], and wet deposition in convective clouds [*Mari et al.*, 2000] and in stratiform precipitations [*Giorgi and Chameides*, 1986]. The model was run with emissions taken from *Dentener et al.* [2004] for the period June to August 2004 and also a realistic daily biomass burning emission inventory of North American forest fires [*Pfister et al.*, 2005]. The transport was forced with analysis from the Meteo France ARPEGE model [*Courtier*, 1991]. A detailed evaluation of the model against observations during ICARTT was presented by *Bousserez et al.* [2007] and a validation of the climate version by *Teyssèdre et al.* [2007]. The modeled CO showed good agreement with the measurements during the period of the plume sampling on the 18 July with a peak at 6 km although the gradients are smoothed out due to too much diffusion (see Figure 1).
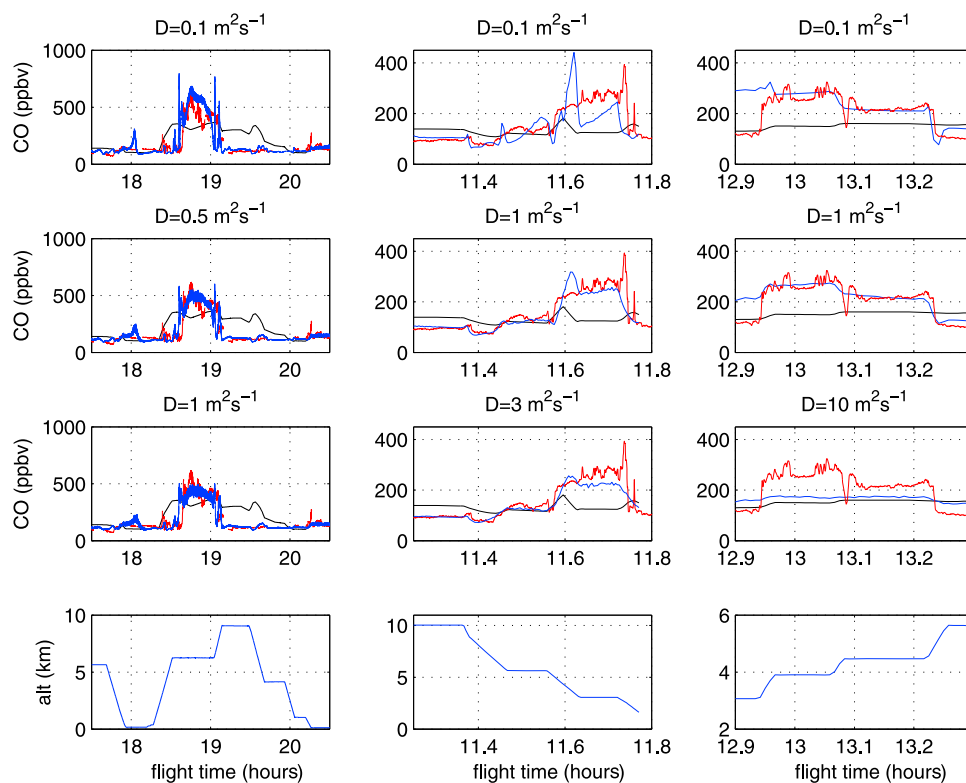
3. Diffusive Ensemble Reconstructions

[13] Turbulent mixing in a stratified atmosphere originates mostly from vertical displacements, translated in the horizontal direction by the natural tracer vertical/horizontal aspect ratio which depends on the ratio between vertical wind shear and horizontal strain [*Haynes and Anglade*, 1997]. This concept was applied originally to the stratosphere but is also relevant to the stratified and layered part of the troposphere [*Newell et al.*, 1999]. In order to estimate dispersion or mixing rates in the midlatitude troposphere we have performed diffusive reconstructions on the same polluted plume on both sides of the Atlantic. The tracer reconstructions were carried out for the Lagrangian match segments of the DC8 and DLR Falcon flights discussed in 2.1.

[14] A range of values of D_v was applied to the vertical displacement of the parcels. CO concentrations were averaged over N parcels arriving at each measurement point along the flight track (with $N = 1000$) and thus represent an average over the different origins of the air parcels.

3.1. Estimates of D_v in Midlatitude Troposphere

[15] On 18 July 2004, the NASA DC8 aircraft flew north into the plume at 7 km and south out of plume at 10 km. The reconstructed CO concentrations with different values of D_v are plotted in the first column of Figure 1 with D_v ranging from 0.1 m² s⁻¹ to 1 m² s⁻¹ . The ensembles are composed of $N = 1000$ particles per point and the duration of backward integration is 96 hours. In all cases, the peak of CO mixing ratio associated with the plume is correctly located near 19.0 UT. The sharpest gradient, and hence the position of the border of the plume, is shifted by about 3 minutes of flight time in the reconstructions with respect to the measurements, which is less than 50 km. This distance is less than half of the horizontal grid size of the advecting wind fields, and errors of this order are likely to result from interpolation errors in horizontal advection. The

Figure 1. In the three upper rows the blue curves show CO mixing ratios reconstructed using ensembles of diffusive backward trajectories as a function of flight time. First column, DC8 flight on 18 July. Second and third columns, Falcon flights on 22 and 23 July, respectively. The in situ measurements are plotted in red and MOCAGE CTM interpolated CO in black in every panel. In the three upper rows, vertical axis represents CO mixing ratio in ppbv and horizontal axis represents flight time (hrs). Rows correspond to values of D_v ranging from 0.1 to 10 m^2 s^{-1}, depending on the flight. The lowest row shows the altitude of the aircraft during the three flights. Time is counted in hours since 00:00 UT on the day of the flight.

sharp gradients of mixing ratio are weakly affected by changes in the diffusivity coefficient D_v of several orders of magnitude (see section 4), whereas the mixing ratio at the peak decreases as the value of D_v increases. A precise estimate of the diffusivity can be obtained by calculating the time integrated CO mixing ratio along the flight track between the entrance and the exit of the plume for different diffusive reconstructions (Figure 2). The integral $\int_{entry}^{exit}[CO]dt$ is a decreasing function of D_v for the reconstructions and interpolating the corresponding quantity for the observations gives the simulated D_v that best fits the observations. The dynamical boundaries of the plume are identified by the extrema in the Lyapunov exponents (see section 4) associated with the two sharp gradients in CO. Figure 2 shows that the best fit is obtained with $D_v \approx 0.35$ m^2 s^{-1}. Notice that the results from all the reconstructions discussed here including this flight show much better agreement with the data than the results from MOCAGE interpolated along the flight tracks. This point is discussed further in section 6.

[16] During the flight on 22 July, the DLR Falcon encountered a divided Alaskan forest fire plume off the Spanish coast. The complex structure of the plume on that day has already been noticed from AIRS CO retrievals [*McMillan et al.*, 2008]. The aircraft entered the plume at 6.5 km and exited it at 2.5 km. Lagrangian reconstructions

with vertical diffusivities ranging from 10^{-1} m^2 s^{-1} to 3 m^2 s^{-1} are shown in the second column of Figure 1. The large peak in CO followed by a ramp obtained with $D = 0.1$ m^2 s^{-1} is far from the observations. Higher values of D redistribute vertically and horizontally CO within the gap between the peak and the ramp. By a criterion similar to that applied to the first column, integrating CO between 11.4 UT and 11.7 UT, Figure 2 shows that $D_v \approx 2.7$ m^2 s^{-1} provides the best fit.

[17] The third column in Figure 1 shows diffusive reconstructions of the plume remnant on 23rd July over France as observed by the DLR Falcon. The sharp gradients observed in the profile on the borders of the plume are associated with changes in altitude of the aircraft. These transitions are present in the reconstructions even if the absolute values do not match measurements very well. The two observed CO plateaus at 275 and 220 ppbv are best reproduced for the second panel with $D_v \approx 1$ m^2 s^{-1} but there is weak sensitivity of the reconstruction to D between 0.1 and 1 m^2 s^{-1}, especially for the second plateau. It is necessary to use very large dissipation (10 m^2 s^{-1}) to produce homogeneous CO concentrations during the sampling. The reconstructed value near 12.9 UT is sensitive to dissipation but is also sensitive to the badly defined initialization of CO in the lowest layers and gives thus a qualitative indication of a large value of D
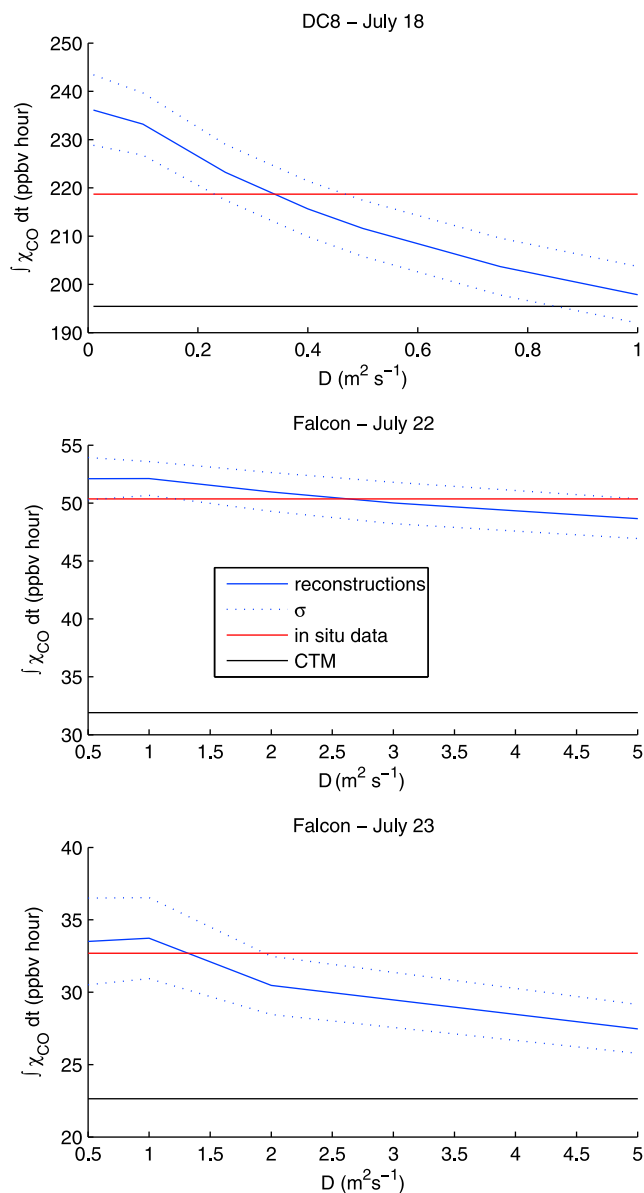
Figure 2. Time integrated CO between the entrance and exit of the plume, as indicated in the text, for observed data and for reconstructions as a function of D. Corresponding flights are indicated above each panel.

at 3 km, which is not totally surprising since this altitude is close to or within the boundary layer during summer. Figure 2 shows that integrating CO between 12.95 UT and 13.25 UT provides a best fit $D_v \approx 1.3$ m^2 s^{-1}.

[18] From these reconstructions on both sides of the North Atlantic, D_v is estimated to change from 0.35 to 2.7 m^2 s^{-1}. This quantity can be considered as local in the sense that it is valid for a limited range of air parcels sampled by the aircraft at a particular time and describes the effect of small-scale turbulence over the last few days before the measurement. Hence the fairly low dispersion of the results is interesting because it suggests that small-scale turbulence does not induce large fluctuations of mixing over parcels traveling for several days or more. In the reconstructions on 18 July, large variations in the value of D_v have little impact on the gradient at the edge of the plume,

and on 23 July gradients change little with D_v. Also, the estimated diffusivity parameter D_v is larger in the case of the Falcon plume sampling compared to the DC8 sampling 5 days earlier. These differences may be related to the fact that the plume was more fragmented after crossing the Atlantic, and complex spatial patterns favor small-scale mixing. Also, it has been shown that the dynamical situation changed in the middle of the Atlantic during the passage to Europe with a warm conveyor belt moving up from the southwest which was likely to be more turbulent [*Real et al.*, 2007, section 5.3]. This resulted in a change in direction in the transport pathway, and is consistent with a larger value of the diffusivity parameter over the eastern Atlantic. Differences in the integration time (4 days compared to 8−9 days) were not found to be important in this case (see next subsection).

3.2. Uncertainties in the Lagrangian Reconstructions

[19] The first important source of error is the representation of advective transport. Small errors in the calculation of the origin position of the parcels may imply large differences in the interpolated mixing ratios from the global model. Even if the model represents accurately the tracer gradients and concentrations in different air masses, inaccurate trajectories could still lead to interpolation of, for example, clean background values instead of plume values and an underestimation in concentrations along the reconstructed flight segment. Adding diffusion prevents spurious fluctuations due to chaos but does not prevent errors due to biases in the analyzed winds. Low dispersion in the cloud of parcels associated with a particular measurement point increases this error, and a whole flight segment may show a fake tracer structure. If dispersion in the ensemble of parcels is large, this effect is reduced. In practice, advection errors depend on the representation of regional and synoptic flow structures in the ECMWF analysis.

[20] As mentioned in the previous section, other sources of error could be related to the length of the runs and the number of parcels. Since this forest fire case is an initial value problem, the length of the run is constrained by the time elapsed between the flights and the emissions. As for the sensitivity of tracer fluctuations to the size N of the ensemble of parcels, it is proportional to $N^{-1/2}$. Previous work has shown that, depending on the time interval of the simulations along the flight track, results with N = 100, 500, 1000 give good results in terms of reproducing of small-scale features [*Legras et al.*, 2005; *Pisso and Legras*, 2008]. See also Figure 1 in Real et al. (submitted manuscript, 2009).

[21] Chemical transformations in air masses are not taken into account in this paper. For CO, we expect this to be reasonably small as shown by *Real et al.* [2007]. See also the discussion in Real et al. (submitted manuscript, 2009).

[22] The main source of errors is certainly relying on MOCAGE outputs to initialize the value of CO within parcels up to 9 days before sampling. The values of CO predicted by MOCAGE depend on many factors including the emissions, the boundary layer representation and the convective scheme.

[23] In order to assess the error in the estimate of diffusivity D, we have performed reconstructions initializing CO values with MOCAGE outputs between 14 July and 3 days before the sampling every 6 hours for the DC8 and

every 24 hours for Falcon flights. The integral of CO has then been calculated as indicated in previous subsection and the standard deviation has been estimated for each value of D. The dotted curves in Figure 2 are constructed by adding and removing this standard deviation to the solid blue curve. It is visible that the only accurate determination of D is obtained on 18 July with a value $D = 0.35 \pm 0.5$ m^2 s^{-1} and that the two other dates lead only to an order of magnitude estimate. The mean reason is the lack of sensitivity of the CO integral to the value of D in these two latter cases, presumably linked to the fragmented nature of the plume at those dates.

4. Tracer Gradient Formation, Long-Range Transport, and Local Dynamical Barriers

[24] An interesting feature of the observed distribution of CO during the flight of 18 July is that the sharp gradient on the plume edge is not dependent on diffusivity. This suggests a recent, strong and localized stretching event that separated the parcels and created a sharp boundary, not yet smoothed by turbulent diffusion.

[25] Regions of high dispersion in the flow (i.e., rapid separation of parcels) are characterized by maxima in Lyapunov exponents [*Pierrehumbert and Yang*, 1993] which describe the transformation of an infinitesimal spherical cloud surrounding a particle into an ellipsoid in a local reference frame relative to the parcel.

[26] Nondiffusive ensembles of back trajectories were initialized along the track of 18 July DC8 flight, to investigate the origin of the air masses and to estimate the stirring using the finite three-dimensional Lyapunov exponents (see *Benettin et al.* [1980] and *Legras et al.* [2005] for details of method). Figure 3 shows the correlation between sharp tracer gradients, rapid back trajectory separation and peaks in the leading Lyapunov exponents along the flight tracks.

[27] From Figure 3 (top), the diversity in the origin of air masses measured along the DC8 flight is apparent. Figure 3a shows that the aircraft penetrated the south side of the plume (as reconstructed from our calculations) and turned back without crossing it. The compact shape of the plume near New Founland is in agreement with AIRS CO retrieval [*McMillan et al.*, 2008]. A first separation of the backward trajectories occurs within the first two days between a branch remaining at midlatitudes and another branch rapidly advected northward within a jet streak with winds above 50 degrees at 300 hPa that extends over northern Canada. This separation is associated with the step in latitude and longitude at time 19.15 UT (in hours from 00:00 the day of the flight) as shown in Figure 3b and c. No change in altitude is associated with this separation as seen from Figure 3d. A step in altitude is produced, however, at a later stage (96 hours, red curve in Figure 3d) at 18.6 UT and 19.05 UT between parcels remaining near the tropopause, and those advected backward within the updraft south to the entrance of the jet streak. The descending parcels (Figure 3d) sample the polluted air near the smoke emissions as seen in Figure 3e, and correspond to the high values of CO reconstructed in Figure 3e.

[28] The reconstructed CO curve fits very well the observations after a shift of 3 minutes along the flight track, that is 50 km in distance, due to the advection errors. This matching indicates that the peak of CO at time 19.1 UT in the reconstruction is spurious. Since it arises from parcels that remained near the tropopause, it is likely to be due to an overestimate of vertical transport of pollution by MOCAGE.

[29] The Lyapunov exponents (Figure 3f) exhibit smaller values inside the reconstructed polluted plume than outside, showing that there was low dispersion inside the plume, preserving it for a fairly long time. Extrema of the largest (positive) and smallest (negative) Lyapunov exponents are associated with the edges of the reconstructed plume. Large absolute values are also associated with the first separation in latitude and are seen outside the plume before 18.6 UT, indicating multiple stretching events in the region. Similar observations and conclusions hold for the case of DLR Falcon flight on 23 July (not shown).

[30] Hence this analysis shows that fast separation by synoptic-scale transport, marked by peaks in the Lyapunov exponents, is the main cause of steep gradients in the tracer fields. Since back trajectories sampling the plume originate from altitudes of 4 km or lower, there is no need to evoke deep convection penetrating the upper troposphere to explain the observations as suggested by *Damoah et al.* [2006].

5. Comparison With Other Diffusivity Estimates and Decay Rates

[31] Previous estimates of D_v in the troposphere are limited. *Schumann et al.* [1995] made an estimate (0.6 m^2 s^{-1} on average) based on dispersion of aircraft plumes using a Gaussian framework which appears to be consistent with the results presented here. Estimates of the effect of small-scale unresolved motion should not be confused with estimates of diffusion obtained by averaging motion over mesoscale and synoptic-scale events [*Hegglin et al.*, 2005]. This is a large-scale limit, in the Taylor sense, which can only match by chance the effect of small-scale diffusion considered here.

[32] In fact, most previous studies focused on the estimation of total or horizontal diffusivity D_h in the troposphere. In stratified flows, without convection, vertical and horizontal diffusion are not independent processes but two aspects of the same phenomenon. For this reason, we have also reconstructed the CO data for 18 July using horizontal instead of vertical stochastic perturbations. The results with ($D_h = 10^3$ m^2 s^{-1}, $D_h = 10^4$ m^2 s^{-1}, $D_h = 10^5$ m^2 s^{-1}), shown in Figure 4 suggest that reconstructions using a value of $D_h = 10^4$ m^2 s^{-1} give the best agreement with the measurements, in this case. These results for the free troposphere can be compared with previous estimates of $D_h = 1 - 5 \times 10^4$ m^2 s^{-1} [*Gifford*, 1982; *Sillman et al.*, 1990; *Mauzerall et al.*, 1998]. Results from these studies are somewhat larger than our estimates but were determined for plumes pollution plumes close to the source regions in or near the boundary layer. In these cases, mixing is likely to have been governed by small-scale turbulence with little influence from large-scale advection. This differs from the fire plume case studied here where transport was governed by synoptic advection and by the strain (as measured by the Lyapunov exponents of the flow), rather than local diffusion. In contrast, smaller values of 5×10^3 m^2 s^{-1} were obtained by *Waugh et al.* [1997] for the stratosphere which can be
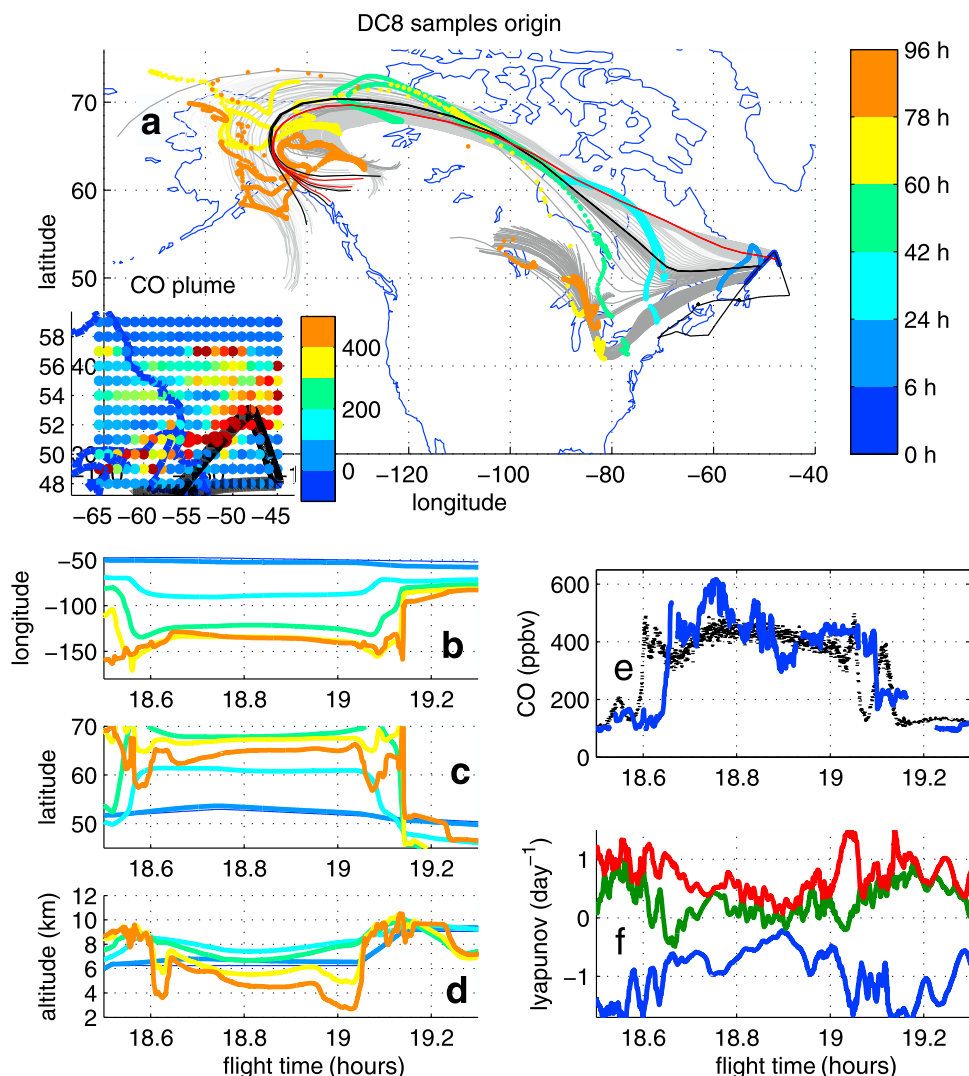
Figure 3. (a) Nondiffusive back trajectories released along flight track during 18 July DC8 match segment are plotted in gray. The previous positions of the parcels are indicated as colored dots. The colors indicate the time counted backward from 19 July 2004 at 12:00 UT as indicated by the bar chart on the right. The red and black trajectories were released at the edge of the plume. The insert in the lower left of this panel shows a map of reconstructed CO at 410 hPa near the flight track with the color shown in the attached bar chart indicated mixing ratio in ppmv. (b) Longitude, (c) latitude, and (d) altitude of the backward positions of the parcels along trajectories as a function of release time along the flight track, using the same color code as in Figure 3a. (e) CO measurements (blue) and diffusive CO reconstructions for $D = 0.5 \, \text{m}^2 \, \text{s}^{-1}$ (black). (f) The three three-dimensional Lyapunov exponents calculated over a 5-day interval: red for the largest, green for the intermediate, and blue for the smallest. Large values of the Lyapunov exponents are associated with rapid separation of backward trajectories and coincide with large tracer gradients.

expected given the higher stability in this region of the atmosphere.

[33] It is interesting here to see how our calculations also compare to estimates of decay rates of chemical mixing ratio. It is apparent that turbulent diffusion smooths out small-scale structures created by the dynamics, limiting the strength of the gradients, and the size of the filaments but it is not easy to derive a general relation for the decay rate. In the simple case of a two-dimensional patch of tracer submitted to uniform strain λ and a turbulent diffusion D_h, the width of the patch is bounded below by $\sqrt{\frac{D_h}{\lambda}}$. Its length is stretched as $e^{\lambda t}$ and its maximum mixing ratio

decays to background concentration as $e^{-\lambda t}$ as a consequence of conservation. In real flows, the relation between stretching and decay rate is somewhat more complicated because shear dominated flows, like the atmosphere, are much less efficient at stirring and mixing than idealized pure strain and the Lyapunov exponent is only an upper bound of the decay rate. Nevertheless, the mixing properties are, on the average, independent of the underlying small-scale diffusion [*Shuckburgh and Haynes*, 2003; F. d'Ovidio et al., A climatology of local mixing events in the upper troposphere and lower stratosphere, submitted to *Journal of Atmospheric Science*, 2009]. For the forest fire plume case examined here, previous studies estimated decay rates
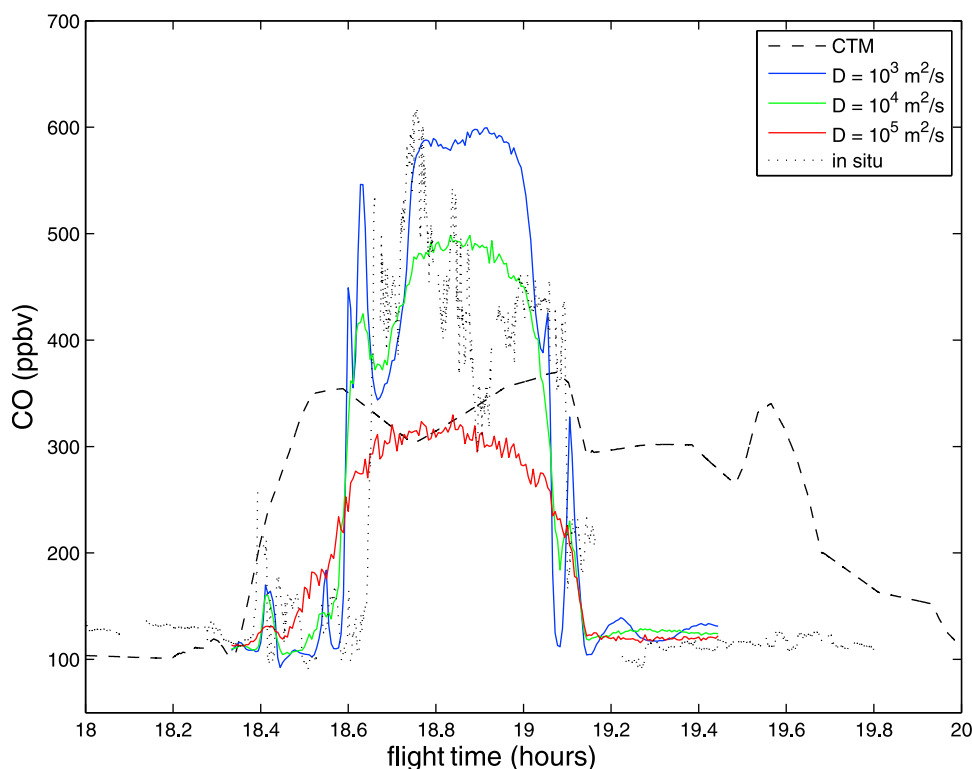
Figure 4. Diffusive reconstructions of DC8 CO on 18 July 2004 with horizontal instead of vertical stochastic perturbations. Black points correspond to in situ CO data; the black dashed line represents the direct interpolation of MOCAGE CO along the flight track at 18:00UT. Blue, green, and red lines represent diffusive ensemble reconstructions with purely horizontal stochastic perturbations corresponding to diffusivities D_h of 10^3, 10^4, and 10^5 m^2 s^{-1}, respectively.

between 0.1 and 0.2 day^{-1} [*Real et al.*, 2007; *Arnold et al.*, 2007]. This can be compared directly to the Lyapunov exponents of the DC8 transect which exhibit values ranging from 0.1 day^{-1} inside the smoke plume to 1 day^{-1} outside as seen in Figure 3f. Values for the Falcon transects are of the same order of magnitude and are also consistent with previous estimates [*Real et al.*, 2007; *Arnold et al.*, 2007]. The latter are point-wise estimations and large variability can be expected from the values of strain inside a folded air mass like the one studied here.

[34] Following the approach of *Haynes and Anglade* [1997] and *Young et al.* [2007], the square root of the quotient D_h/D_v can be used to estimate the aspect ratio of tracer structures induced by shear and strain, in this case for the free troposphere. Using an upper limit $D_h = 10^4$ m^2 s^{-1} and estimated values $D_v = 0.35 - 1$ m^2 s^{-1} gives aspect ratios in the range of 100 to 170 for this case. These values are slightly smaller than the value 200 previously estimated for the stratosphere [*Haynes and Anglade*, 1997].

## 6. Relation to Three-Dimensional CTMs

[35] In this section, we use the diffusivities obtained in this study to estimate the spatial resolutions required to accurately simulate pollutant plume transport and dispersion in the free troposphere using global CTMs. Although such models employ sophisticated advection schemes for tracer transport [e.g., *Prather*, 1986; *Williamson and Rasch*,

1989], the solution of the advection-diffusion problem results in numerical diffusion which depends on model temporal and spatial resolutions. Comparison of the diffusivities derived here for the DC8 case and MOCAGE results interpolated along the flight track shows that D_v of 1 m^2 s^{-1} is still too low to match the model results. Examination of Figure 4 also shows that the global model results are equivalent to applying a horizontal diffusivity of at least 10^5 m^2 s^{-1} which is about one order of magnitude greater than the value of D_h giving the best fit with the data. *Tan et al.* [1998] estimated numerical diffusivities of $10^6 - 10^7$ m^2 s^{-1} in a global stratospheric model (SLIMCAT) based on comparison with reconstructed tracer fields using reverse domain filling techniques. Therefore at current horizontal resolutions, numerical diffusivities in global models are much larger than real "physical" turbulent diffusivities which are ignored.

[36] In contrast, diffusion is parameterized in mesoscale models as a function of the scale of spurious numerical waves and certain schemes are based on dynamical parameters. For example, the Smagorinsky deformation closure can be used to estimate the resolution needed to represent an effective D_h. As an example, the horizontal diffusivity in MM5 [*Grell et al.*, 1995] is written as

$$D_h = D_{h0} + \frac{1}{2}k^2\Delta x^2 S$$
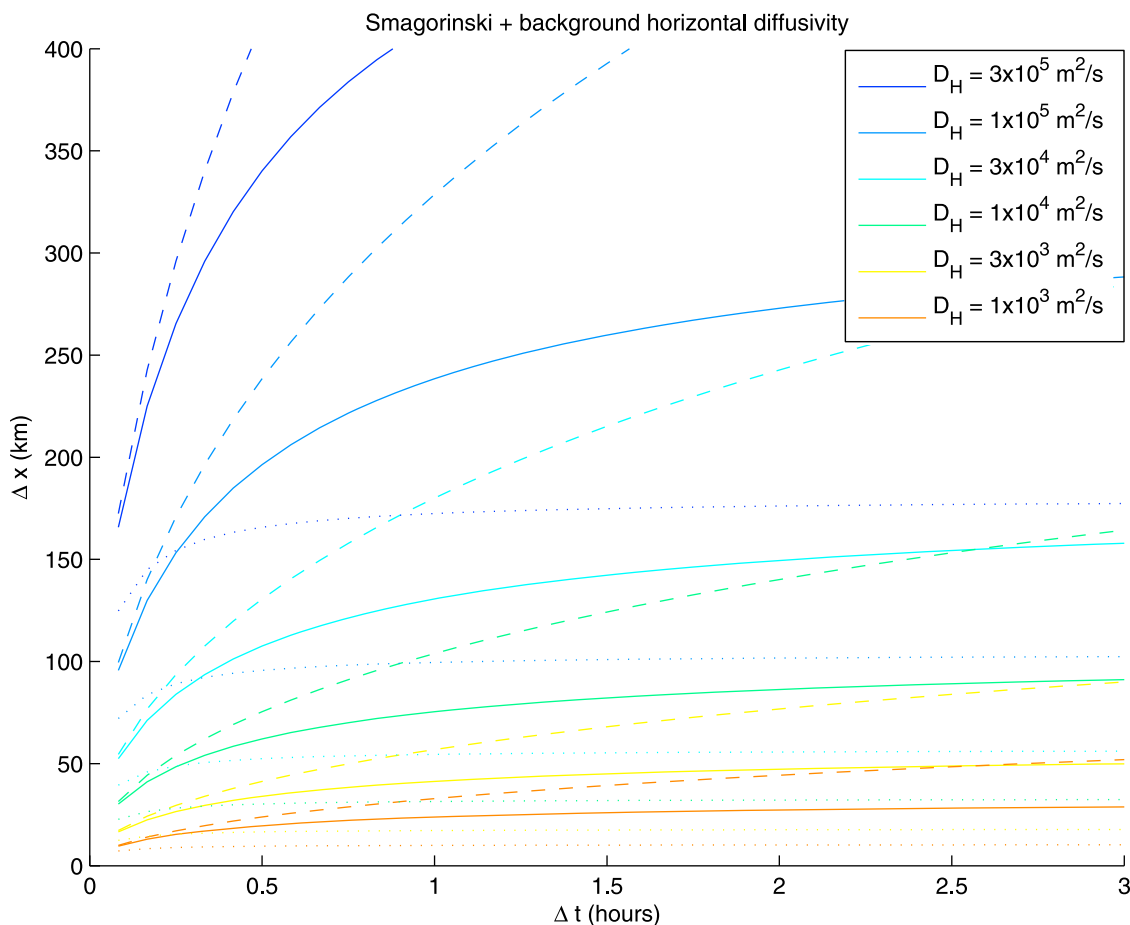
Figure 5. Relationship between time and space resolutions corresponding to different values of horizontal diffusivity estimated using a mesoscale (MM5) model setup and shears of 0.1, 1, and 10 day^{-1} (dashed, solid, and pointed lines, respectively). MOCAGE parameters yield a horizontal diffusivity above 10^5 m^2 s^{-1}. See text for details.

where $k = 0.4$ is the von Karman constant, $S = \left[\left(\frac{\partial u}{\partial x} - \frac{\partial v}{\partial y} \right)^2 + \left(\frac{\partial v}{\partial x} + \frac{\partial u}{\partial y} \right)^2 \right]^{1/2}$ represents shear induced diffusion [*Smagorinski*, 1963] and $D_{h0} = K \frac{\Delta x^2}{\Delta t}$ is the basic diffusivity related to the model resolution in space and time, needed in mesoscale models to control nonlinear instability and numerical aliasing. The constant K is user defined [*Xu et al.*, 2000] and its default value in MM5 is 3×10^{-3} [*Grell et al.*, 1995].

[37] The order of magnitude of the Smagorinsky closure can be approximated by using the Lyapunov exponents calculated in this study by approximating the shear with the Lyapunov exponent $S \approx \lambda$. The relation between the spatial and temporal resolution for a certain diffusivity is given by:

$$\Delta x = \sqrt{D_h \Delta t \left(K + \frac{1}{2} k^2 \lambda \Delta t \right)^{-1}}$$

[38] These calculations suggest (see Figure 5) that a global CTM like MOCAGE with a dynamical time step of 1 hour and 15 minutes for subgrid processes requires a horizontal grid of $\Delta x \approx 40$ km or less to reach the values of $D_h \approx 10^4$ m^2 s^{-1} estimated in this study. This estimate is based on a typical λ of 1 day^{-1}, more information can be found in Figure 5. Since the plume transport in the case studied here was collected during a flow regime with reduced zonal distortion, it is likely that smaller values of Δx are needed in more complex situations.

[39] The optimal vertical/horizontal balance in spatial resolution is also important. The vertical and horizontal resolutions applied in the MOCAGE runs (800 m vertical and 220 km horizontal) give an aspect ratio of 1:275. The estimates presented above, together with the aspect ratios derived in section 5 (100–170), suggest that in order to capture long-range transport of pollutant plumes, global models need to be run at horizontal resolutions of less than ~40 km and vertical resolutions of 500 m or less. Note that studies of observed layers in the free troposphere suggest a median layer thickness of around 500 m [*Thouret et al.*, 2000, 2001]. At these resolutions, it may also be necessary to include parameterizations of horizontal and vertical diffusion in global models. It is also worth noting that while previous studies investigating the impact of resolution on photochemistry showed rather small effects down to 110 km [e.g., *Wild and Prather*, 2006], results presented in the

companion paper (Real et al., submitted manuscript, 2009) show this is not always the case and that significant errors can occur at higher resolutions.

7. Conclusions and Outlook

[40] We have studied the dynamical evolution of a forest fire plume during long-range transport in order to quantify mixing and dispersion in the free troposphere. The plume was sampled several times, by the DC8 aircraft on the 18 July and again by the DLR Falcon on the 22 and 23 July 2004. For the first time in the troposphere, stochastic Lagrangian reconstructions of CO concentrations were used to estimate vertical and horizontal turbulent diffusivity coefficients, D_v and D_h during matching flight segments across the plume. The vertical turbulent diffusivity D_v ranges between 0.35 and 2.7 m^2 s^{-1} and the horizontal diffusion D_h upper bound is of the order of 10^4 m^2 s^{-1}. These values represent subgrid processes in the standard spatial resolution of operational centers like ECMWF and are consistent with previous, albeit rather limited, estimates of D_h and D_v. The use of analyzed meteorological winds yielded a small shift in the location of gradients in the reconstructed profiles. Analysis of the results, together with further calculations of the Lyapunov coefficients showed that strain and stretching of the flow were largely responsible for keeping the plume intact during transport in the first few days from the fire region (when it was sampled by the DC8), and over the western Atlantic. A developing low pressure system over the eastern Atlantic led to more dispersion (and higher D_v) of the plume when it was sampled by the DLR Falcon over Europe. Also, interestingly, explicit convective parameterizations were not required, in this case, for the calculation of vertical displacements of the trajectories with significant vertical motion taking place over the region of the fires in Alaska using information in the analysis alone, in contrast to previous studies [*Damoah et al.*, 2006]. Lyapunov exponents, which are a measure of the strain which generally controls tracer decay rates inside a plume, were used to derive in-plume decay rates between 0.1 and 1 day^{-1}. These values are comparable to results from previous studies of decay or mixing rates based on exponential decay of a tracer (CO) to background concentrations. Our results were also used to provide estimates of the aspect ratio of tropospheric tracer structures of the order of 100–170 in the free troposphere.

[41] We also used our results to estimate that the numerical diffusion related to coarse resolution of the MOCAGE model runs used in this study to be larger than 10^5 m^2/s, which is at least one order of magnitude larger than the value estimated from the reconstructions of the in situ measurements. The results suggest that the resolution required for the accurate simulation of long-range transport of pollutant plumes in the free troposphere and their dispersion is less than 40 km in the horizontal and 500 m in the vertical. These values provide an upper bound which will need to refined once global models are run at sufficient resolutions with suitable parameterizations for horizontal and vertical diffusion. Note that, here we only consider resolutions required for accurate dynamical transport of pollutant plumes in the free troposphere where advection is dominant.

Nonlinearities in the chemistry, particularly at plume edges, may require even higher resolutions (see Real et al., submitted manuscript, 2009).

References

Arnold, S. R., et al. (2007), Statistical inference of OH concentrations and air mass dilution rates from successive observations of nonmethane hydrocarbons in single air masses, *J. Geophys. Res.*, *112*, D10S40, doi:10.1029/2006JD007594.

Bechtold, P., E. Bazile, F. Guichard, P. Mascart, and E. Richard (2001), A mass flux convection scheme for regional and global models, *Q. J. R. Meteorol. Soc.*, *127*, 869–886.

Benettin, G., G. Galgani, L. Giorgilli, and J. Strelcyn (1980), Lyapunov characteristic exponents for smooth dynamical systems and for hamiltonian syastems; a method for computing all of them: I. Theory, *Meccanica*, 9–80.

Bousserez, N., et al. (2007), Evaluation of the MOCAGE chemistry transport model during the ICARTT/ITOP experiment., *J. Geophys. Res.*, *112*, D10S42, doi:10.1029/2006JD007595.

Colette, A., and G. Ancellet (2006), Variability of the tropospheric mixing and of streamer formation and their impact on the lifetime of observed ozone layers, *Geophys. Res. Lett.*, *33*, L09808, doi:10.1029/2006GL025793.

Cook, P. A., et al. (2007), Forest fire plumes over the north atlantic: p-TOMCAT model simulations with aircraft and satellite measurements from the ITOP/ICARTT campaign, *J. Geophys. Res.*, *112*, D10S43, doi:10.1029/2006JD007563.

Courtier, P. (1991), The arpege project at Meteo-France, in *Workshop on Numerical Methods in Atmospheric Models*, vol. 2, pp. 193–231, Eur. Cent. for Med.-Range Weather Forecasts, Reading, U. K.

Crowther, R., K. S. Law, D. M. Pyle, J. A. Pyle, S. Bekki, and H. G. J. Law (2002), Characterising the effect of large-scale model resolution upon calculated OH production using MOZAIC data, *Geophys. Res. Lett.*, *29*(12), 1613, doi:10.1029/2002GL014660.

Damoah, R., et al. (2006), A case study of pyro-convection using transport model and remote sensing data, *Atmos. Chem. Phys.*, *6*, 173–185.

Dentener, F., D. Stevenson, J. Cofala, R. Mechler, M. Amann, P. Bergamaschi, F. Raes, and R. Derwent (2004), The impact of air pollutant and methane emission controls on tropospheric ozone and radiative forcing: CTM calculations for the period 1990–2030, *Atmos. Chem. Phys.*, *4*, 8471–8538.

Edouard, S., B. Legras, F. Lefèvre, and R. Eymard (1996), The effect of small-scale inhomogeneities on ozone depletion in the Arctic, *Nature*, *384*, 444–447.

Esler, J. G., G. J. Roelofs, and M. O. Köhler (2004), A quantitative analysis of grid-related systematic errors in oxidising capacity and ozone production rates in chemistry transport models, *Atmos. Chem. Phys.*, *4*, 1781–1795.

Fehsenfeld, F., et al. (2006), International Consortium for Atmospheric Research on Transport and Transformation (ICARTT): North America to Europe: Overview of the 2004 summer field study, *J. Geophys. Res.*, *111*, D23S01, doi:10.1029/2006JD007829.

Gifford, F. (1982), Horizontal diffusion in the atmosphere: A Lagrangian dynamical theory, *Atmos. Environ.*, *16*, 505–512.

Giorgi, F., and W. L. Chameides (1986), Rainout lifetimes of highly soluble aerosols and gases as inferred from simulations with a general circulation model, *J. Geophys. Res.*, *91*, 14,367–14,376.

Grell, G., J. Dudhia, and D. Stauffer (1995), A description of the Fifth-Generation Penn State/NCAR Mesoscale Model MM5, *Tech. Rep. NCAR/TN-398+STR*, Natl. Cent. for Atmos. Res., Boulder, Colo.

Hall, T., and D. Waugh (1997), Tracer transport in the tropical stratosphere due to vertical diffusion and horizontal mixing, *Geophys. Res. Lett.*, *24*, 1383–1386.

Haynes, P., and J. Anglade (1997), The vertical-scale cascade in atmospheric tracers due to large-scale differential advection, *J. Atmos. Sci.*, *54*, 1112–1136.

Hegglin, M., D. Brunner, T. Peter, J. Staehelin, V. Wirth, P. Hoor, and H. Fischer (2005), Determination of eddy diffusivity in the lowermost stratosphere, *Geophys. Res. Lett.*, *32*, L13812, doi:10.1029/2005GL022495.

Josse, B., P. Simon, and V.-H. Peuch (2004), Radon global simulations with the multiscale CTM MOCAGE, *Tellus*, *56B*, 339–356.

Lefèvre, F., G. P. Brasseur, I. Folkins, A. Smith, and P. Simon (1994), Chemistry of the 1991–1992 stratospheric winter: Three dimensional model simulations, *J. Geophys. Res.*, *99*, 8183–8195.

Legras, B., B. Joseph (2003) and F. Lefèvre,, Vertical diffusivity in the lower stratosphere from Lagrangian back-trajectory reconstructions of ozone profiles, *J. Geophys. Res.*, *108*(D18), 4562, doi:10.1029/2002JD003045.

Legras, B., I. Pisso, F. Lefèvre, and G. Berthet (2005), Variability of the Lagrangian turbulent diffusion in the lower stratosphere, *Atmos. Chem. Phys.*, *5*, 1605–1622.

Louis, J.-F. (1979), A parametric model for vertical eddy-fluxes in the atmosphere, *Boundary Layer Meteorol.*, *17*, 187–202.

Mari, C., D. J. Jacob, and P. Bechtold (2000), Transport and scavenging of soluble gases in a deep convective cloud, *J. Geophys. Res.*, *105*, 22,255–22,267.

Mauzerall, D., et al. (1998), Photochemistry in biomass burning plumes and implications for tropospheric ozone over the tropical south atlantic, *J. Geophys. Res.*, *103*, 8401–8423.

McKenna, D., P. Konopka, J.-U. Grooß, G. Günther, R. Müller, R. Spang, D. Offermann, and Y. Orsolini (2002), A new Chemical Lagrangian Model of the Stratosphere (CLaMS): 1. Formulation of advection and mixing, *J. Geophys. Res.*, *107*(D16), 4309, doi:10.1029/2000JD000114.

McMillan, W. W., et al. (2008), AIRS views transport from 12 to 22 July 2004 Alaskan/Canadian fires: Correlation of AIRS CO and MODIS AOD with forward trajectories and comparison of AIRS CO retrievals with dc-8 in situ measurements during INTEX-A/ICARTT, *J. Geophys. Res.*, *113*, D20301, doi:10.1029/2007JD009711.

Methven, J., S. Arnold, F. O'Connor, H. Barjat, K. Dewey, J. Kent, and N. Brough (2003), Estimating photochemically produced ozone throughout a domain using flight data and a Lagrangian model, *J. Geophys. Res.*, *108*(D9), 4271, doi:10.1029/2002JD002955.

Methven, J., et al. (2006), Establishing Lagrangian connections between observations within air masses crossing the Atlantic during the International Consortium for Atmospheric Research on Transport and Transformation experiment, *J. Geophys. Res.*, *111*, D23S62, doi:10.1029/2006JD007540.

Newell, R. E., V. Thouret, J. Y. N. Cho, P. Stoller, A. Marenco, and H. G. Smit (1999), Ubiquity of quasi-horizontal layers in the troposphere, *Nature*, *398*, 316–319.

Nho-Kim, E.-Y., M. Michou, and V.-H. Peuch (2004), Parameterization of size dependent particle dry deposition velocities for global modeling, *Atmos. Environ.*, *38*, 1933–1942.

Pfister, G., P. Hess, L. Emmons, J. Lamarque, C. Wiedinmyer, D. Edwards, G. Petron, J. Gille, and G. Sachse (2005), Quantifying CO emissions from the 2004 Alaskan wildfires using MOPITT CO data, *Geophys. Res. Lett.*, *32*, L11809, doi:10.1029/2005GL022995.

Pierrehumbert, R. T., and H. Yang (1993), Global chaotic mixing on isentropic surfaces, *J. Atmos. Sci.*, *50*, 2462–2480.

Pisso, I., and B. Legras (2008), Turbulent vertical diffusivity in the subtropical stratosphere, *Atmos. Chem. Phys.*, *8*, 697–707.

Prather, M. J. (1986), Numerical advection by conservation of second-order moments, *J. Geophys. Res.*, *91*, 6671–6681.

Pyle, J. A., and A. M. Zavody (1990), The modelling problems associated with spatial averaging, *Q. J. R. Meteorol. Soc.*, *116*, 753–766.

Real, E., et al. (2007), Processes influencing ozone levels in Alaskan forest fire plumes during long-range transport over the North Atlantic, *J. Geophys. Res.*, *112*, D10S41, doi:10.1029/2006JD007576.

Schumann, U., P. Konopka, R. Baumann, R. Busen, T. Gertz, H. Schlager, P. Schulte, and H. Volkert (1995), Estimate of diffusion parameters of aircraft exhaust plumes near the tropopause from nitric oxide ond turbulence measurements, *J. Geophys. Res.*, *100*(D7), 14,147–14,162.

Shuckburgh, E., and P. H. Haynes (2003), Diagnosed transport and mixing using a tracer-based coordinate system, *Phys. Fluids*, *15*(11), 3342–3357, doi:10.1063/1.1610471.

Sillman, S., L. Logan, and S. Wofsy (1990), A regional scale model for ozone in the United States with subgrid representation of urban and power plant plumes, *J. Geophys. Res.*, *95*, 5731–5748.

Smagorinski, I. (1963), General circulation experiments with the primitive equations. I. The basic experiment, *Mon. Weather Rev.*, *91*(3), 99–163.

Stockwell, W. R., F. Kirchner, M. Khun, and S. Seefeld (1997), A new mechanism for regional atmospheric chemistry modelling, *J. Geophys. Res.*, *102*, 25,847–25,879.

Stohl, A., O. Cooper, and P. James (2004), A cautionary note on the use of meteorological analysis fields for quantifying atmospheric mixing, *J. Atmos. Sci.*, *61*, 1446–1453.

Stohl, A., C. Forster, A. Frank, and G. Wotawa (2005), Technical note: The Lagrangian particle dispersion model flexpart version 6.2, *Atmos. Chem. Phys.*, *5*, 2461–2474.

Tan, D., P. H. Haynes, A. MacKenzie, and J. Pyle (1998), Effects of fluid-dynamical stirring and mixing on the deactivation of stratospheric chlorine, *J. Geophys. Res.*, *103*, 1585–1605.

Teyssèdre, H., et al. (2007), The climatic version of the MOCAGE tropospheric-stratospheric chemistry and transport model: Description, evaluation and sensitivity to surface processes, *Atmos. Chem. Phys.*, *7*, 5815–5860.

Thouret, V., J. Cho, R. Newell, A. Marenco, and H. Smit (2000), General characteristics of tropospheric trace constituent layers observed in the MOZAIC program, *J. Geophys. Res.*, *105*, 17,379–17,392.

Thouret, V., J. Cho, M. Evans, R. Newell, M. Avery, J. Barrick, G. Sachse, and G. Gregory (2001), Tropospheric ozone layers observed during PEM-Tropics B, *J. Geophys. Res.*, *106*, 32,527–32,538.

Waugh, D., et al. (1997), Mixing of polar vortex air into middle latitudes as revealed by tracer-tracer scatterplots, *J. Geophys. Res.*, *102*, 13,119–13,134.

Wild, O., and M. J. Prather (2006), Global tropospheric ozone modeling: Quantifying errors due to grid resolution, *J. Geophys. Res.*, *111*, D11305, doi:10.1029/2005JD006605.

Williamson, D. L., and P. J. Rasch (1989), Two-dimensional semi-Lagrangian transport with shape-preserving interpolation, *Mon. Weather Rev.*, *117*, 102–129.

Wu, S., L. J. Mickley, D. J. Jacob, J. A. Logan, R. M. Yantosca, and D. Rind (2007), Why are there large differences between models in global budgets of tropospheric ozone?, *J. Geophys. Res.*, *112*, D05302, doi:10.1029/2006JD007801.

Xu, M., J. Bao, T. Warner, and D. Stensrud (2000), Effect of time step size in MM5 simulations of a mesoscale convective system, *Mon. Weather Rev.*, *129*, 502–516.

Young, W., P. Rhines, and C. Garrett (2007), Shear flow dispersion, internal waves and horizontal mixing in the ocean, *J. Phys. Oceanogr.*, *12*, 515–527.

———————————

J. L. Attié, Laboratoire d'Aérologie (UMR 5560), Université de Toulouse/CNRS, 14 Avenue Edouard Belin, 31400 Toulouse, France.

N. Bousserez, Department of Physics and Atmospheric Science, Dalhousie University, Halifax, NS, B3H 3J5, Canada.

K. S. Law, Service d'Aéronomie (LATMOS, UMR 7620), CNRS/IPSL/Université Pierre et Marie Curie, 4 place Jussieu, 75252 Paris Cedex 05, France.

B. Legras, Laboratoire de Météorologie Dynamique (UMR 8539), CNRS/IPSL/Ecole Normale Supérieure, 24, Rue Lhomond, F-75231 Paris Cedex 05, France.

I. Pisso, Department of Applied Mathematics and Theoretical Physics, Centre for Mathematical Sciences, University of Cambridge, Wilberforce Road, Cambridge CB3 0WA, UK. (i.pisso@damtp.cam.ac.uk)

E. Real, CEREA, Ecole Nationale des Ponts et Chaussées, 6-8 Avenue Blaise Pascal, Cité Descartes Champs-sur-Marne, 77455 Marne la Vallée, Paris Cedex 2, France.

H. Schlager, Institut für Physik der Atmosphäre, Deutsches Zentrum für Luft und Raumfahrt, Operpfaffenhofen, D-82234 Wessling, Germany.